International Journal of Applied Engineering Research ISSN 0973-4562 Volume 13, Number 14 (2018) pp. 11392-11401

Plenoptic Imaging for Object Detecting and Tracking: An Edge Detection Approach

Yessaadi Sabrina

PG Scholar
Department of Mathematics and Computer Science,
University Center Abdelhafid Boussouf. Mila, Algeria,
Badji Mokhtar University.Annaba, Algeria,

Laskri Mohamed Tayeb

Professor
Department of Computer Science,
Badji Mokhtar University.Annaba. , Algeria,

Abstract

Object detection in machine vision and image processing has gained increasing interest due to its social and security potential. Earlier measurement methods suffer from drawbacks due to the complexes scene properties (geometrics, illuminations, etc.). To improve upon these limits, new optical methods have been proposed. One of these methods was the plenoptic imaging. It is a promising optical technique, that furnishes substantial information of the object image or a full 3D scene. In fact, this technique captures information on a light fields imaging of the appropriate scene and records them in a single shot. Computed location and the propagation direction information of the object light are used as efficient descriptors to detect and track the object displacement. In this work, we propose a novel approach to detect objects in light fields images, based on the image representation with the first and the second order derivative, well known as Gradient and Laplacian image descriptors. These obtained images are used in a correlation process to detect localize and track an object in an image scene.

Keywords: Light fields, Laplacian, Gradient, Edge detection, Correlation.

INTRODUCTION

As a crucial technique in computer vision and image processing, object detection has often been used for object segmentation and tracking for computer vision systems. It is based on the detection of instant objects like human body, face, car, bicycles, or buildings. This approach plays an important role in visual surveillance applications, pedestrian detection and tracking, image retrieval, and face recognition.

Earlier measurement methods suffer from drawbacks due to complexes scene properties (geometrics, illumination, ..., etc.). To improve these limits, new optical methods for describing objects are efficiently and largely invaded in computer vision and machine learning. Quite recently, considerable attention has been paid to plenoptic imaging, this approach captures information on the three-dimensional light field of appropriate scene and records, simultaneously, the location information and the propagation direction of the object light plane [1,2]. These computed measures are used as efficient descriptors to detect and track moving objects [3,4].

In this paper, we propose a new sensing strategy for object detection and tracking based on, first, the extraction of visual information of a frame image such as a discrete object, specifically: edges. At this level, we focus on the description of light field images based on the detection and the localization of significant intensity variation, or what it is called: edge. This will be performed using the first and the second derivative, well known as Gradient and Laplacian. The edge image will use to detect and localize the object in the image scene, by performing a correlation process.

RELATED WORKS

Edge detection is a long-standing problem in computer vision. It is an important phase for several computer vision and image processing techniques, as pattern recognition, image segmentation, image matching, object detection and tracking. This method aims to locate pixels of high variation in intensity from the other neighbor's pixels [5,6].

In the graphics community, successful approaches have been proposed to perform the object detection process, based on edge detection, under a variety of condition scene and camera constraints. See D. Ziou and S. Tabbone, in [6], for an interesting overview of researches in this field. Certain of these methods proved very good model accuracy in the two-dimension image plane, therefore their great challenges are the object moving and the background changes.

However, existing solutions suffer from many underlying assumptions, due to complexes scene properties (geometrics, illumination, ..., etc.). Recently computer vision community has converged in using light field imaging as a new representation of the image scene. The light field imaging, or, as Gortler et al called the Lumigraph [7], are 4-dimensional images containing both, orientation, and position information of each point of the object [8,9]. Effectively, Light field imaging record the 3D Information of the scene in the image plane, this information is represented by the location of the individual light rays, that is defined by the position coordinates and the propagation direction of the incoming light, defined by the incidence angles [1,2].

As a new technique, the light field was largely used for several technologies of computer vision and image processing [9], object detection was one of these techniques. Although, few works were presented for object detection, using the light

field image. Efficient but few techniques were proposed, in literature.

In their work, Donald. G Dansereau et al proposed a framework to detect changes in mobile light field cameras [9]. A. Shimada, H. Nagahara, and R. I. Taniguchi used the light field for object detection, their method generates an arbitrary in-focus plan and an out-focus one that filled the background region. The object detection is used for video surveillance, too, and performed by computing the viewpoint of spatial-temporal light field consistency to processing the light rays [3].

In a second work, Shimada et al presented a new change detection strategy using light rays, they determine in-focus and an out-focus area, by generating an active surveillance field. The evaluating of the focusses defines light rays source. The temporal changes are captured by the update of the light ray's background [10].

Using light field image and the property of the 4D plenoptic function, as depth information, it can be useful to provide the metric to the foreground and background separation. for more details see the work of Kevin Boyle [11].

By far, nearly all existing edge detection algorithms used images provided by a regular camera. In our proposed method we use a different kind of image representation: the light field image, which provides high-quality 2D images, using their different views. That will be used to compute the edge position pixel. The edge detection task is performed by the computing of the first and the second derivative as known as the Gradient and the Laplacian operators, respectively. These two operators furnish the edge image that will be used to detect an object based on the correlation and a matching algorithm.

For the matching algorithm, we used the correlation technique. As an old technique in mathematics and statistics, correlation technique was used to define and measure the dependence between two or several random variables.

In image processing, Digital Image Correlation or DIC was used as an effective and efficient measurement tool for templates matching in image and object deformation and tracking. DIC is based on numerical computation performed on digital image processing to measure image deformation and object displacement. This measurement is evaluated by various correlation criterions known as the coefficients of correlation. In his work, B. Pan proposed a review paper, that resumes the most used correlation criteria. Pan demonstrates that there are three robust and efficient correlation criterions: the zero-mean normalized cross-correlation (ZNCC) criterion, the ZNSSD, zero-mean normalized sum of squared difference criterion and a parametric zero-mean normalized sum of squared difference (PSSDab) criterion, with two unknown parameters a and b [12].

Our DIC process was performed and tested using all correlation criterions proposed by Pan in his Survey. However, we choose the ZNCC as an example for this paper. Our model was tested using the Stanford 3D scanning repository- Synthetic Light Field Archive. This database is a part of Stanford light field database. It contains 19 subsets describing 19 objects for each subset. Based on two-plane light field parameterization, the subset database contains image view spaced in either 5x5 or 7x7 views of different 3D scenes. All light fields are rendered as Portable Network Graphics images (.png).

THE LIGHT FIELD IMAGING

In his notebook, Leonardo Davinci described the body of the air "as a set of full of an infinite number of radiant pyramids caused by the objects located in it" [8]. The radiant pyramids referee above is what we called the light field. The light field is described as: "a set of rays passing through any point in space", these rays are different in sense of orientation and intensity [1,8].

In "Thoughts on Ray Vibrations", Michael Faraday proposes to interpret light as a field. The term of the light field was, firstly introduced and defined, in 1936, by Gershun, in his book: The Light Field, Translated into English by Parry Moon and Gregory Timoshenko [8,13,14].

Light fields imaging is a technique that is widely used in recent research. As it used, both, orientation and position of each light provided by the object to describe it. It offers a new image formation, based on multiple view representation approach for images in the real scene.

Light field object models are used to capture and store the appearance of an object from different points of view. They represent objects using their different views and render a photo-realistic view of different kind object shape. A simple interpolation technique can achieve the rendering phase.

A. Definitions

In literature, the light field is defined as a description of the radiance of light rays in 4D space. It describes the image as a field of rays, according to their orientation and their position [1].

The light field is a vector function that describes the amount of light flowing in every direction through every point in space. The direction of each ray is given by the 5D plenoptic function, and the magnitude of each ray is given by the radiance [1].

i. Light Field in 4D

The light field in 4D is defined, using two distant planes: *UV* and *ST*, intersecting the optical axis. The amount of coming light ray at the plane *UV*, through the plane *ST*, is defined by the 4-Dimensional plenoptic function *LF (u, v, s, t).*

Where: (*u, v)* and *(s, t)* denote, respectively, the distance between the two planes *UV* and *ST* from the optical axis [1,2,8].

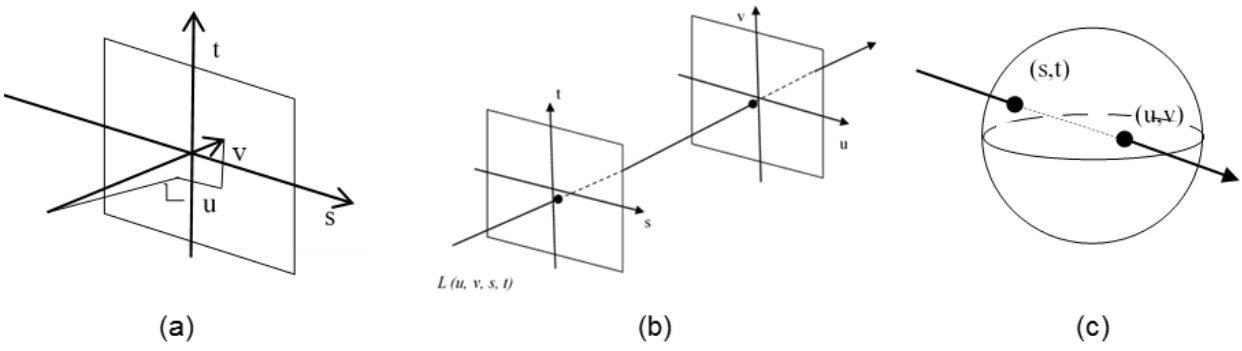

Figure 1. Light filed parametrization

ii. The light field in 2D

The light field in 2D is defined, using two distant planes: U and S, intersecting the optical axis. The amount of coming light ray at the plane U, through the plane S, is defined by the 2-Dimensional plenoptic function LF *(u, s).* Where *u* and *s* denote, respectively, the distance between the two planes *U* and *S* from the optical axis.

B. *Light Field parametrization*

The parametrization of a 4D set of rays has three different descriptions. The light rays see Figure 1a, two planes, that is illustrated in Figure 1b and the spherical representation, Figure 1c. The most used is based on the definition of ray's coordinates using 2 planes in a random position, see Figure 1b.

That parametrization made a special definition of the light field: as a collection of perspective images positioned on the first plane, let it be *ST*, and projected into the second plane, the *UV* plane. Each perspective is taken from the well-defined position of the observer [1,9]. In our work, we will use the light field in 2D space, as a basic definition to perform our experiment phase.

C. The plenoptic function

The 5D plenoptic function describing "everything that can be seen" with references to psychophysical and physiological literature on vision [8]. It was called the "photic field" by Parry moon, pat Hanraha and Levoy, give it the name of the 4D light field [1, 8].

i. Definition

The plenoptic function is the dubbed name of the radiance along unchanging light rays arrangement in a 3D space. As a function it describes the cats light coordinates: x, y, z, and the angles ɵ and ϕ. if we assume that radiance is constant along an empty space, the Plenoptic function will be defined as a 4-D function.

Edge Detection and Derivative Functions

Based on the discontinuity property in the image intensity, the edge can describe the line as an edge segment, which the intensity value of their pixels is lower or higher than the one at the background, on each side [4,15].

Differentiation is an appropriate way to determine this discontinuity in an image. It can be expressed by the calculation of partial derivatives of the discrete function representing the image intensity [7]. The definition of the image by the first derivative (the gradient) or the second derivative (the Laplacian) has been widely used, to describe the image in terms of its outlines. This representation is efficient, as it is an optimal representation of the image basing, only, on its significant descriptors.

A. First derivative and the Gradient of an intensity image

The gradient of an image has a very important property, it always points in the direction of the greatest rate of change of the intensity at the location (x, y). As a vector, two parameters may describe the gradient, these two descriptors are the magnitude and the direction [7].

i. Mathematical definition.

For a function of intensity values, I (x, y), the gradient, at (x, y) position, is defined as the two-dimensioned column vector ∇I, where:

$$\nabla I \equiv Grad(I) \equiv \begin{pmatrix} G_x \\ G_y \end{pmatrix} \quad (1)$$

Where

$$G_x \equiv \frac{\delta I(x,y)}{\delta x} \quad (2)$$

$$G_y \equiv \frac{\delta I(x,y)}{\delta y} \quad (3)$$

B. Geometrical properties of the gradient.

i. The gradient magnitude.

The gradient magnitude denotes the rate of change in the direction of the gradient vector, at a given location. this magnitude computes a length of the gradient vector:

$$Mag\,(x,y) = Mag(\nabla I) = \sqrt{G_x^2 + G_y^2} \tag{4}$$

For more suitable computation, the magnitude in equation (4), can be approximated by absolute values of G_x and G_y, as followed:

$$Mag(x,y) \approx |G_x| + |G_y| \tag{5}$$

ii. The gradient orientation.

The computing of the angle gives the gradient vector orientation as followed:

$$\theta = tan^{-1}\left(G_x / G_y\right) \tag{6}$$

In case of G_y is equal to zero at the (x, y) position, the angle θ is equal to Π/2 if G_x is positive or -Π/2 else.

C. Gradient and first order derivatives.

The approximation of the first derivative can be computed using a different kind of masks, the major characteristics of these masks are that the sum of their coefficients is always equal to zero, which means, in constant intensities, the mask will give a response of zero [7]. this corresponds to the definition of derivatives. Using the notation in Table 1, the image I (x, y) denotes the 3x3 image pixel, p_5 is pixel with (x, y) location. p_1 denotes the location x-1, y-1, and so on.

Table 1. The region neighborhood

P_1	P_2	P_3
P_4	P_5	P_6
P_7	P_8	P_9

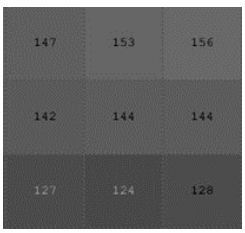

The filters in which we are interested are the Sobel mask operators, masks of 3x3 size, that presented in Table 2. At each (x, y) position of pixel p, the approximation in the x-direction is obtained by the sum of the third and the first row of the 3x3 image region neighborhood, implemented by the mask of Table 2a, and the approximation in the y-direction is obtained by the sum of the third and the first column of the 3x3 image region implemented by the mask of Table 2b.

Table 2. The Sobel mask operators

-1	-2	-1
0	0	0
1	2	1

(a)

-1	0	1
-2	0	2
-1	0	1

(b)

Using the 3x3 neighborhood of p_5 center, the approximations of G_x (x, y) and G_y (x, y) is obtained are as follow [7]:

$$G_x(x,y) = (p_7 + 2*p_8 + p_9) - (p_1 + 2*p_2 + p_3) \tag{7}$$

$$G_y(x,y) = (p_3 + 2*p_6 + p_9) - (p_1 + 2*p_4 + p_7) \tag{8}$$

i. Gradient vector Properties.

The gradient magnitude and orientation can be computed using the substitution of G_x (x, y) and G_y (x, y) of the equation 7 and 8 in the equation 5. The magnitude and the orientation image, at each point of (x, y) position are computed as below:

$$Mag(x,y) \approx |(p_7 + 2*p_8 + p_9) - (p_1 + 2*p_2 + p_3)| + |(p_3 + 2*p_6 + p_9) - (p_1 + 2*p_4 + p_7)| \tag{9}$$

And the orientation, defined by the angle θ is computer using the following equation:

$$\theta = tan^{-1}\left(\frac{(p_7 + 2*p_8 + p_9) - (p_1 + 2*p_2 + p_3)}{(p_3 + 2*p_6 + p_9) - (p_1 + 2*p_4 + p_7)}\right) \tag{10}$$

In Figure 2, Figure 2a, Figure 2b and Figure 2c, show, respectively, the original, the magnitude, and the orientation gradient images obtained using equations 9 and 10.

(a) (b) (c)

Figure 2. The magnitude image and the orientation of gradient image

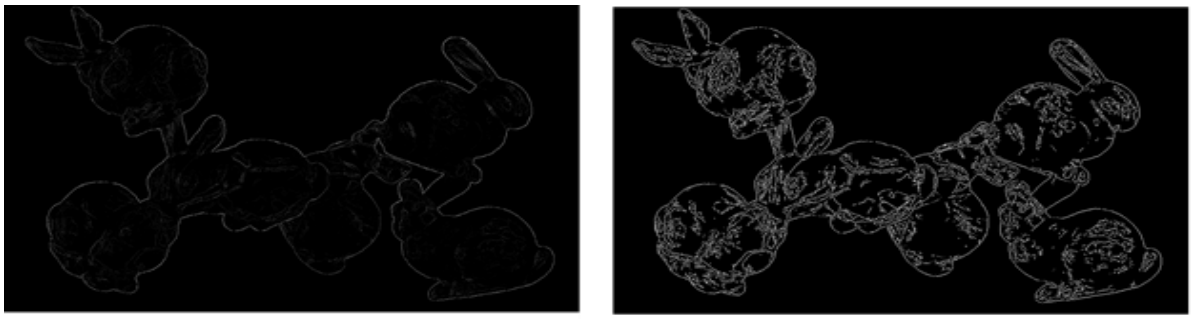

(a). Before thresholding *(b). After thresholding*

Figure 3. The edge image using Gradient operator

D. Non-Maxima Suppression Algorithm

Optimal edge operator would have marked points belonged to edge line as a maximum. To find these point positions, we have to non-maximum suppress the magnitude gradient image, through the gradient direction of each of their points [15].

In equation 11 and 12, we estimate, as an example, the value of the magnitude of a point situated between p (x, y+1) and p (x+1, y+1). The value of interpolated magnitude gradient is computed using these following two equations:

$$G_1 = \frac{G_x}{G_y} * G(x+1, y+1) + \left(1 - \frac{G_x}{G_y}\right) * G(x, y+1) \quad (11)$$

$$G_2 = \frac{G_x}{G_y} * G(x-1, y-1) + \left(1 - \frac{G_x}{G_y}\right) * G(x, y-1) \quad (12)$$

We mark the point p (x, y) as maximum if

G (x, y) > G_1 and G (x, y) > G_2, and its magnitude value will be equal to 255 (white pixel) else, it's value will be zero (black pixel).

The values of the orientation angle belong to the interval value of [-π/2, π/2[.

Figure 3 shows the obtained edge detector image, Figure 3a before thresholding phase, and Figure 3b after the thresholding algorithm.

E. Second Derivative for Image Representation

In what follows, we will use the representation of the image by the Laplacian operator.

i. Laplacian and the second derivative of an image.

The Laplacian is an isotopic derivation operator (invariant to the rotation of the image), and linear (calculated from the derivation which is a linear operation) [7].

The Laplacian of a function f is calculated as follows:

$$\nabla^2 f = \frac{\partial^2 f}{\partial x^2} + \frac{\partial^2 f}{\partial y^2} \quad (13)$$

In image processing, the expression (13) is expressed in a discrete form, using pixel intensity values, in a well-defined neighborhood in the picture.

The definition of the second, partial and directional derivatives according to x and y are expressed by the following equations:

$$\frac{\partial^2 f}{\partial x^2} = f(x+1, y) + f(x-1, y) - 2 * f(x, y) \quad (14)$$

$$\frac{\partial^2 f}{\partial y^2} = f(x, y+1) + f(x, y-1) - 2 * f(x, y) \quad (15)$$

And so, the Laplacian is obtained by summing equations (14) and (15), as follows:

$$\nabla^2 f = f(x+1, y) + f(x-1, y) + f(x, y+1) + f(x, y-1) - 4 * f(x, y) \quad (16)$$

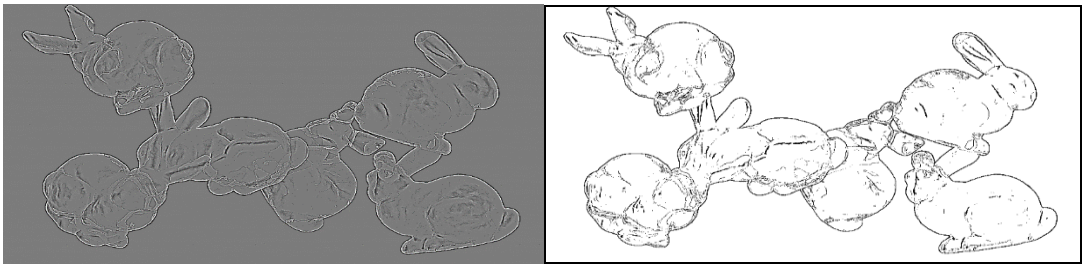

(a) Before thresholding (b) After thresholding

Figure 4. The edge image using Laplacian operator

EXPERIMENTAL RESULTS

Computing using the equations 16, Figure 4a and Figure 4b show, respectively, the obtained Laplacian image before and after thresholding.

Object Detection and digital Image Correlation

Detection and tracking of objects in images is an important phase in the object recognition process. One of the techniques allowing the realization of this task is the correlation techniques.

A. Definition of the correlation

Proposed in mathematics by Karl Pearson in 1896, the correlation is defined as a similarity measure quantity to be calculated. Mathematically, the correlation is defined by the product of two functions, representing two signals [16].

i. Mathematical definition.

The following mathematical formula defines this calculation:

$$\mathrm{Cor}(x,y) = \frac{\mathrm{cov}(x,y)}{\sigma_x * \sigma_y} \tag{17}$$

Where:

Cor (x, y): represents the degree of correspondence between the variables x and y, it is also called the linear correlation coefficient of Pearson.

Cov (x, y): is the covariance matrix of the variables x and y. ∂_x and ∂_y are the standard deviations of the two variables.

The covariance matrix and the standard deviations of the variables x and y are calculated as follows:

$$\mathrm{Cov}(x,y) = \frac{1}{M}\sum_{i=1}^{M}(x-\bar{x}) * (y_y - \bar{y}) \tag{18}$$

$$\sigma_x = \sqrt{\frac{1}{M}\sum_{i=1}^{M}(x_i-\bar{x})^2} \tag{19}$$

$$\sigma_y = \sqrt{\frac{1}{M}\sum_{i=1}^{M}(y_i-\bar{y})^2} \tag{20}$$

Where $\bar{x}$ and $\bar{y}$ represent the mean of, respectively, the values of the variables x and y of size M.

ii. The coefficient of linear correlation

The coefficient of linear correlation takes values between -1 and 1, its absolute value measures the intensity of the linear connection between the data. The variables are strongly correlated positively or negatively if this absolute value of the correlation coefficients is closed to 1, but, if the value of the coefficient of correlation is closed to 0, the variables are independent [12,17].

iii. Zero Mean Normalized Cross-correlation criterion (ZNCC)

Correlation is a local operation, sensitive to changes in intensity pixels of the image. In influence on the value of the correlation coefficient, the change of this characteristic can provide false correlation results.

To perform the correlation phase, we used, as mentioned before, the Zero Mean Normalized Cross Correlation Criterion (ZNCC). It is the most used in research works, characterized by its robust and efficiency results. The ZNCC criterion is Invariant to the scale and offsets changes of the image [18].

B. Experimental phase

For our experimental phase, we use the definition of the ZNCC, according to the following formula:

$$\mathrm{Cor}_{I,g}(x,y) = \frac{1}{L_g * C_g * \sigma_I(x,y) * \sigma_g}\sum_{l=-L_g/2}^{L_g/2}\sum_{k=-C_g/2}^{C_g/2}\left(\left(I(x+l,y+k)-\mu_I(x,y)\right)-\left(g(l,k)-\mu_g\right)\right)^2 \tag{21}$$

Where μ_g and are σ_g the mean and the variance of the sub-image, μ_I [m, n] and σ_I [m, n] are the mean and the variance of the image calculated at each iteration browsing the image I with the sub-image g. These parameters are computed using the following formulas [18]:

$$\mu_g = \frac{1}{L_g C_g} \sum_{l=-L_g/2}^{L_g/2} \sum_{k=-C_g/2}^{C_g/2} g(l,k) \quad (22)$$

$$\sigma_g = \sqrt{\frac{1}{L_g C_g} \sum_{l} \sum_{k} (g(l,k) - \mu_g)^2} \quad (23)$$

$$\mu_I(m,n) = \frac{1}{L_g C_g} \sum_{l=-L_g/2}^{L_g/2} \sum_{k=-C_g/2}^{C_g/2} I(m+l, n+k) \quad (24)$$

$$\sigma_I(m,n) = \sqrt{\frac{1}{L_g C_g} \sum_{l} \sum_{k} (I(m+l, n+k) - \mu_I(m,n))^2} \quad (25)$$

C. Examples and results

As mentioned above, images used in the tests are images from the Stanford 3D scanning repository-synthetic light field archive, specifically the subset named: DragonAndBunnies. Only perspective views of a light field are used in this light field set.

In our tests, we used 500 different images. and the results mentioned in the reports are those of the following image and sub-image, illustrated in Figure 5:

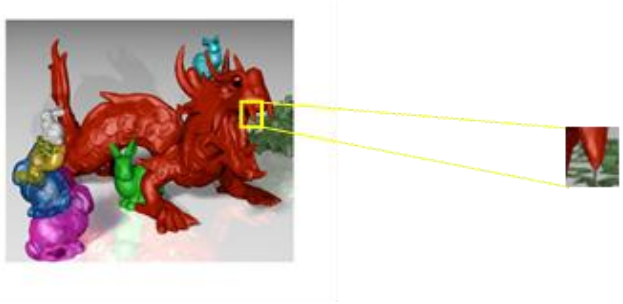

Figure 5. Image and sub-image used in the test

Figure 6a and Figure 6b show the ZNCC-correlation image between the original image and sub-image. results concern gradient and Laplacian images.

These correlation images are different in terms of intensity values pixels, this is due to different definitions and representations of using images. However, the correlation result is the same in term of the position of the maximum correlation value. Whatever the image representation, the pixel of the maximum value of the ZNCC criterion is unique, this pixel has a gray level equal 255 (white pixel). This value is unique and corresponds to the maximum value of the ZNCC coefficient (equals to 1).

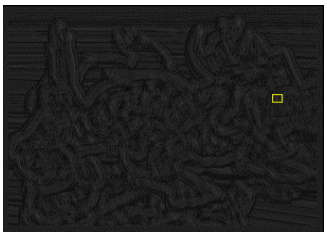

(a). Gradient image

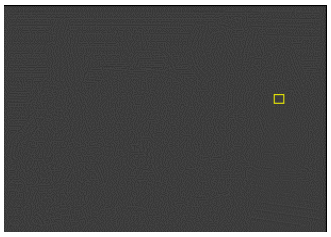

(b). Laplacian image

Figure 6. The image correlation with ZNCC

i. Identical maximum correlation pixel

If the object belongs to the image, the pixel with the maximum correlation value is detected in the same position. In the case of our example, the pixel with the maximum intensity value is unique and is detected at the position x = 244 and y = 720. See Figure 7.

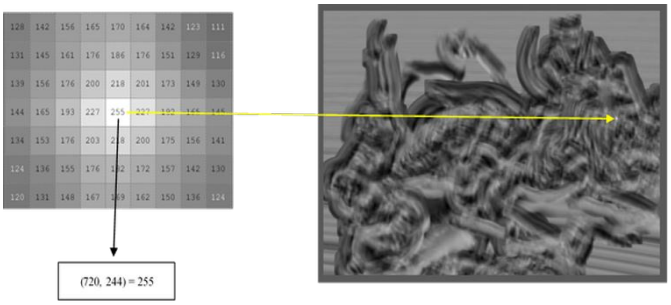

Figure 7. The correlation image with sub-image

The corresponding wireframe mesh representation of the three image representations are illustrated in Figure 8. The color is proportional to surface height or the pixel intensity value.

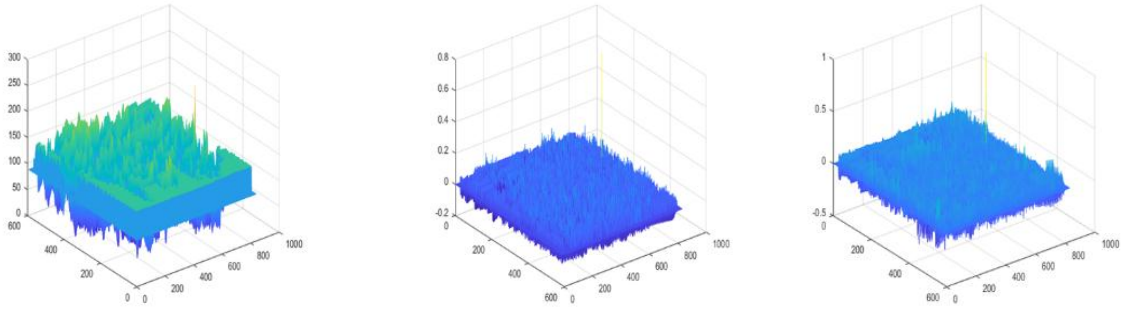

(a). Simple image (b). Gradient image (c). Laplacian image

Figure 8. The wireframe mesh representation of image correlation

ii. The Invariance of ZNCC

To test the insensitivity of the ZNCC coefficient to the scale and the offset changes, we have compared the image with a sub-image that belonged to another perspective view of the light field, in DragonAndBunnies database. The object was detected in the image, whenever it was extracted from another perspective view of the image light field. The object is detected in at, slight different coordinates, X= 248 and Y=717. Figure 9 illustrates the obtained result.

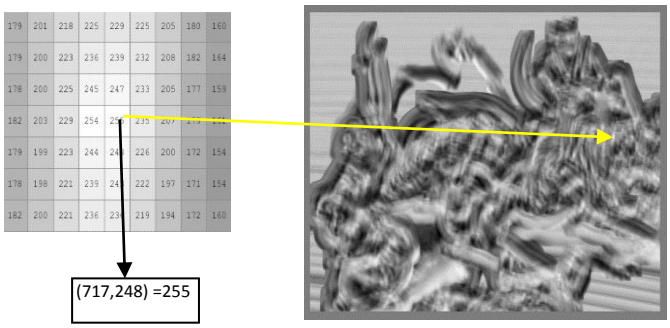

Figure 9. The correlation image with a sub-object of another perspective view image

The correspondent wireframe mesh representations are presented throw the Figure 10.

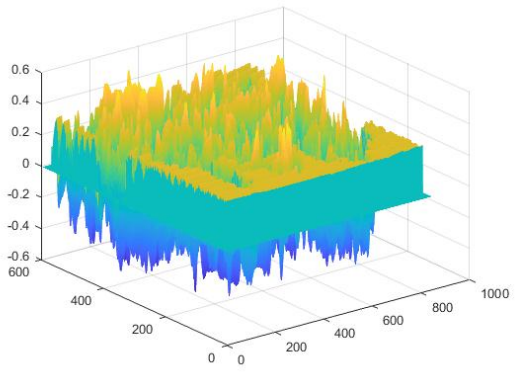

Figure 10. The wireframe mesh representation

CONCLUSION

In this article, we have presented a new object detection technique on light fields images. Our technique is based on the edge description of the image, using the differentiation method.

Throw multiple experiences, we have shown that working on light field images deal, efficiently, with the object detection process drawbacks. The preprocessing phase will be neglected as we can get high-resolution images, with only special sophisticated cameras. This specificity resolved the problem of sensitivity of the differentiation to the noise. Further denoising algorithms were presented, D. G. Dansereau proposed a very powerful Light Field Toolbox which offers many Matlab scripts about decoding, rectification calibration, color correction and visualization in addition of some linear depth/focus and denoising filter in the last version of the Toolbox.

Indeed, the Stanford 3D scanning repository- Synthetic Light Field Archive was built using powerful methods that produce smooth manifold surfaces by eliminating outliers in the range data and reduce noise in images.

We have proved, during experiments and test that the use of the derivative method of edge detection had performed the edge detection task in terms of optimality representation and efficiency results.

In conclusion, the study has shown the importance of the image representation in an image processing or a computer vision system. And its influences on the time computing and result quality.

FUTURE RESEARCH DIRECTIONS

As an additional material test, we propose to use different image representation, the histogram of oriented gradients (*HOG*), Laplacian of Gaussian (LoG), or an eigenvalues images to perform the edge detection task.

To deal with space color definition. An additional comparison of edge detecting in a light field image represented in the three coordinates L*, a*, and b* with the whole image in the L*a*b* CIE 1976 color space domain. The difference in

results was very significant. Edges obtained with the image represented in L^* and b^* coordinates are more significative than those obtained with a^* and L*a*b* CIE 1976 color space. Figure 11 and Figure 12 demonstrate the influence of color space color for the edge detection process.

Based on this result, we invite researchers to use, other color space representation, following to the image type and application, to perform, as possible, the edge detection process.

The proposed method can be readily used in the medical imaging field, the vessel detection in retinal light field image. Since the difficulties to get a light field image of a fundus in the retinal image. The retinal image can be simulated using optical design tools, like Zemax and Oslo. These tools are very efficient and have been tested for such task. We can site the work proposed by Sha Tong et al. In their work, they simulate the light field fundus photography by using a Zemax tool. The quality of the image of the simulated light field fundus is better than this representing the simple retina image. This high quality used to detect vessel in retinal images.

REFERENCES

[1] Levoy M.: Light fields and computational imaging. Computer, 39(8), 46-55, 2006.

[2] Levoy M., Hanrahan P.: Light field rendering, In Proceedings of the 23rd annual conference on Computer graphics and interactive techniques (pp. 31-42), ACM, August 1996.

[3] Xu Y and Lam M. L, "Light Field Vision for Artificial Intelligence". In Artificial Intelligence and Computer Vision (pp. 189-209), Springer, Cham, 2017

[4] Zobel M., Fritz M., and Scholz I., "Object Tracking and Pose Estimation Using Light-Field Object Models", In VMV (pp. 371-378), November 2002.

[5] Belongie S., Malik J., and Puzicha J.: Matching shapes. In Computer Vision, ICCV 2001, Proceedings. Eighth IEEE International Conference on (Vol. 1, pp. 454-461), 2001.

[6] Ziou D and Tabbone S, "Edge detection techniques-an overview", Pattern Recognition and Image Analysis C/C of Raspoznavaniye Obrazov I Analiz Izobrazhenii, 8, 537-559,1998.

[7] Gonzalez R. C., Woods R. E.: Digital image processing. 2002.

[8] Adelson E. H., Bergen J. R.: The plenoptic function and the elements of early vision, 1991.

[9] Dansereau D. G.: Plenoptic signal processing for robust vision in field robotics, 2013.

[10] Shimada A, Nagahara H and Taniguchi R. I, "Change detection on light field for active video surveillance", In Advanced Video and Signal Based Surveillance (AVSS), 2015 12th IEEE International Conference on (pp. 1-6), IEEE, August 2015.

[11] Boyle Kevin C.: Occluded Edge Detection in Light Field Images for Background Removal.

[12] Gortler S. J., Grzeszczuk R., Szeliski R., and Cohen M. F.: The lumigraph. In Proceedings of the 23rd annual conference on Computer graphics and interactive techniques, pp. 43-54, 1996.

[13] Canny J. F.: Finding edges and lines in images, 1983.

[14] Lewis J. P.: Fast normalized cross-correlation, In Vision interface (Vol. 10, No. 1, pp. 120-123), May 1995.

[15] Gershun A.: The light field, Studies in Applied Mathematics, 18(1-4), 51-151, 1939.

[16] Shimada A, Nagahara H. and Taniguchi R. I, "Object detection based on spatio-temporal light field sensing", Information and Media Technologies, 8(4), 1115-1119, 2013.

[17] Kumar B. V., Mahalanobis A. and Juday R. D.: Correlation pattern recognition. Cambridge University Press, 2005.

[18] Pan B.: Recent progress in digital image correlation, Experimental Mechanics, 51(7), 1223-1235, 2011.

(a) (b) (c) (d)

Figure 11. Gradient edge image using (c) L^*, (a) a^*, (b) b^*, and (d) $L^*a^*b^*$ color space

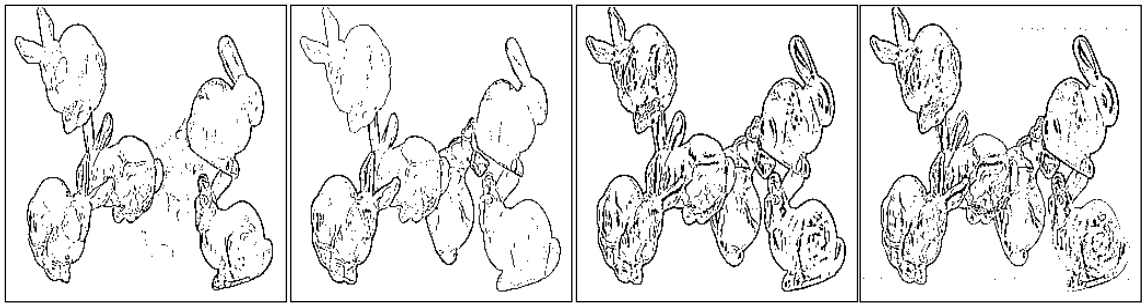

(a) (b) (c) (d)

Figure 12. Laplacian edge image using: (c) L^*, (a) a^*, (b) b^*, and (d) $L^*a^*b^*$ color space